Magnetically driven superhydrophobic meshes with the capacity of moving at the air/water and oil/water interfaces

Jihua Zhang,[a,]* Huadong Feng[a], Weitao Zao[a], Yunfeng Zhao[a], Hui Zhang[b,c,]* and Yibin Liu[b]

[a]Aerospace Research Institute of Material and Processing Technology, Beijing, 100076, P. R. China.

[b]School of Materials Science and Engineering, Tsinghua University, Beijing, 100084, P. R. China.

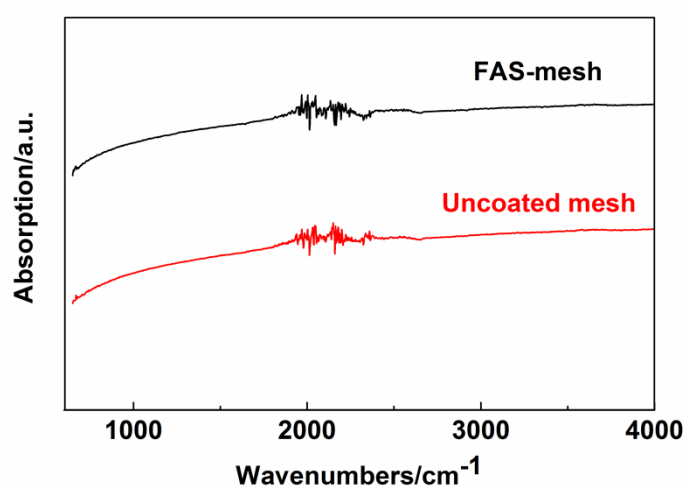[c]Institute of Chemistry, Chinese Academy of Sciences, Beijing, 100190, P. R. China.

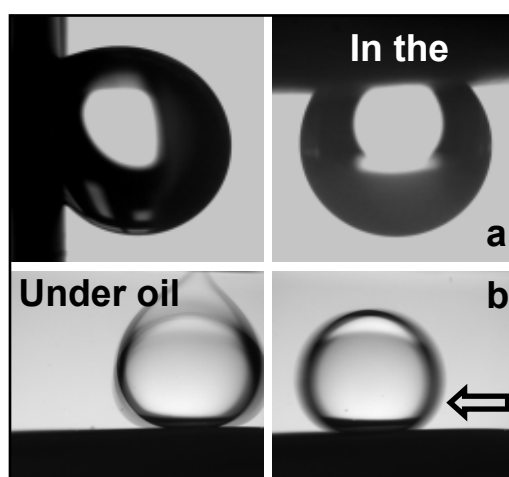**Fig. S1** ATR-FTIR spectrum of uncoated mesh and FAS-mesh, respectively.

Fig. S2 Different adhesion states of water droplet on the mesh when they are placed in the air and under oil: a) High adhesion state in the air. The droplet will attach to the FAS-mesh even if the mesh is turned over. b) Low adhesion state under oil. The droplet can easily roll off from the mesh at low inclination angle of below 5°.
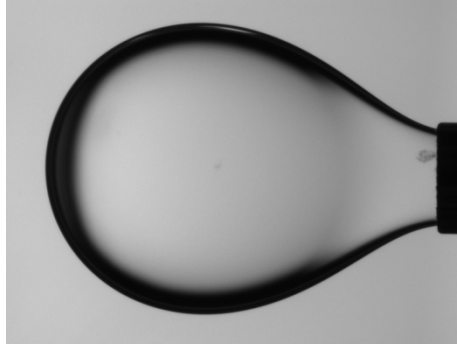
Fig. S3 Optic image of oil/water interface measurement by maximum bubble pressure method

Simple discussions on the trends: the contact angles on the FAS-mesh are increased with the increase of *w* value in our experiment.

It is noticed that the contact angle increases by increasing *w* value in our cases. This result can be well explained by eq. 7: With the increase of *w* value, spacing ratio of $D^*=(d+w)/d$ increases, implying that air or oil fraction improves at the composite interfaces (see Fig. 4b). Then the contact angles on the mesh increase. But the trend is limited by the impalement pressure. Such impalement pressure is determined by *w* values, intrinsic wettability and volume of droplet[1]. When the sale size of *w* value is beyond the range that required by Cassie equation, the trend will change. This means, once the *w* values increase to a certain one (w_c), the contact angles of droplet on the mesh will decrease. Nevertheless, at the range of *w* values (25~100 μm), the increasing trend of contact angle can be seen in our experiments.

The analysis about the phenomena: contact angles under oil are larger than those in air.

The capillary constant (*a*) can be used to express the weight and buoyancy effects on the shapes of the droplet: $a = \sqrt{\dfrac{\gamma}{\Delta\rho g}}$, where γ is the interface tension, $\Delta\rho$ is density difference between oil (or air) and water, *g* is gravitational acceleration. For air/water interface, the value of *a* is approximately 2.7 mm. The shape of droplet is controlled by surface tension on the condition that the droplet radius is less than 2.7 mm (its

volume is less than 82.4 μL). But for the oil/water interface, the a values are 4.0 mm (hexane), 4.46 mm (hexadecane) and 5.45 mm (peanut oil), respectively. This means if the radius of droplet is beyond a value, the gravity or buoyancy force play a role for its shape. In our case, the volume of oil is 4 μL to deposit on the mesh (its radius is far less than the capillary constant), so the contact angle is believed to be the real one controlled by interface tension.

On the other hand, equilibrium contact angle ($\theta_{air,\ w}$) of a water droplet in the air is deduced by Young's equation (see Fig. S4):

$$\gamma_{SG} = \gamma_{SW} + \gamma_{WG} \cos\theta_{air,w} \ (S1)$$

which relates the surface tensions among the three phases: solid, water and gas (air): γ_{WG} is the water/gas tension; γ_{SG} is the solid/gas tension; γ_{SW} is the solid/water tension. For an oil droplet in the air, the Young's equation is re-written:

$$\gamma_{SG} = \gamma_{SO} + \gamma_{OG} \cos\theta_{air,o} \ (S2)$$

where $\theta_{air,\ o}$ is the equilibrium contact angle of an oil droplet.

Similarly, when a water droplet is placed under the oil, the equilibrium contact angle of a water droplet ($\theta_{oil,\ w}$) can be expressed:

$$\gamma_{SO} = \gamma_{SW} + \gamma_{WO} \cos\theta_{oil,w} \ (S3)$$

where γ_{WO} is the water/oil tension; γ_{SO} is the solid/oil tension.

Eq. S2 is transferred:

$$\gamma_{SG} - \gamma_{OG} \cos\theta_{air,o} = \gamma_{SO} \ (S4).$$

Combining eq.S3 with eq. S4 leads to:

$$\gamma_{SG} - \gamma_{SW} - \gamma_{OG} \cos\theta_{air,o} = \gamma_{WO} \cos\theta_{oil,w} \ (S5)$$

The term of γ_{SG} -γ_{SW} at the left side of eq. C5 is replaced by eq. S1:

$$\frac{\gamma_{WG} \cos\theta_{air,w} - \gamma_{OG} \cos\theta_{air,o}}{\gamma_{WO}} = \cos\theta_{oil,w} \ (S6)$$

In order to compare the values between $\theta_{oil,\ w}$ and $\theta_{air,\ w}$, we make the relation: $\Delta\theta = \cos\theta_{oil,w} - \cos\theta_{air,w}$. If $\Delta\theta$ is less than zero, the value of $\theta_{oil,\ w}$ will be more than $\theta_{air,\ w}$. Eq. S6 is introduced to the term of $\Delta\theta$:

$$\Delta\theta = \cos\theta_{oil,w} - \cos\theta_{air,w} = \frac{\gamma_{WG}\cos\theta_{air,w} - \gamma_{OG}\cos\theta_{air,o}}{\gamma_{WO}} - \cos\theta_{air,w} = \left(\frac{\gamma_{WG}}{\gamma_{WO}} - 1\right)\cos\theta_{air,w} - \frac{\gamma_{OG}\cos\theta_{air,o}}{\gamma_{WO}} \quad (S7)$$

In our cases, there are the relations: $\gamma_{WG} > \gamma_{WO}$; $\theta_{air,\ w} > 90°$; $\gamma_{OG}/\gamma_{WO} > 0$; $\theta_{air,\ o} < 90°$. Thus accordingly to eq. S7, the value of $\Delta\theta$ is theoretically less than zero, *i. e.* $\theta_{oil,\ w} > \theta_{air,\ w.}$ This means that the contact angle of a water droplet under the oil is always more than that in the air.
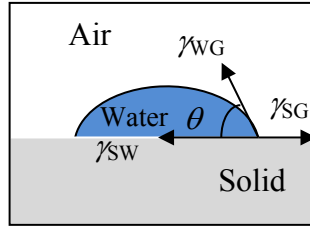

Fig. S4 Schematic of the interface tensions among three phases.

Table S1 Physical parameters of various interfaces

	Air/water	Hexane/water	Hexadecane/water	Peanut oil/water
Interface tension/mN/m	72.8	48	44.8	25
Oil density/g/cm^3	1.000 (water)	0.692	0.770	0.914

Table S2 Element content of uncoated mesh and FAS-mesh from XPS analysis

Samples	Fe$_{2p}$(%)	C$_{1s}$ (%)	O$_{1s}$ (%)	F$_{1s}$ (%)	Si$_{2p}$ (%)	In$_{3d}$(%)	Cr$_{2p}$ (%)
uncoated	2.35	69.51	24.98	0	0	0.3	1.51
FAS-mesh	2.07	52.20	19.74	22.48	2.75	0.03	0.74

Video S1 Micro-robot model always stand at the hexane/water interface when lots of hexane was poured into water.

Video S2 Stability of the micro-robot supported by the FAS-meshes at oil/water interface when it was shocked by hand.

Video S3 Micro-robot model freely moved on water under the permanent magnet when it was floating at the air/water interface in the closed system.

Video S4 Micro-robot model freely rotated on water by the control of magnetic stir when it was floating at the air/water interface in the closed system.

Video S5 Micro-robot model freely moved at hexane/water interface in the closed system when it was guided by the permanent magnet.

Video S6 Micro-robot model freely rotated at hexane/water interface in the closed system when it was guided by the magnetic stir.

Video S7 Micro-robot model freely rotated at hexane/water interface in the open system when it was guided by the magnetic stir.

Video S8 Micro-robot rotated at the hexane/water interface when more hexane was poured and disturbed this interface.

Reference

[1] Xue, Z.; Wang, S.; Lin, L.; Chen, L.; Liu, M.; Feng, L.; Jiang, L. A Novel Superhydrophilic and Underwater Superoleophobic Hydrogel-Coated Mesh for Oil/Water Separation. *Adv. Mater.*, **2011**, *23*: 4270-4273.